Solid Freeform Fabrication 2017: Proceedings of the 28th Annual International Solid Freeform Fabrication Symposium – An Additive Manufacturing Conference
Reviewed Paper

Mechanical performance of selective laser melted 17-4 PH stainless steel under compressive loading

P. Ponnusamy[1, 2], S.H. Masood[1,*], D. Ruan[1], S. Palanisamy[1, 2], R.A. Rahman Rashid[1, 2], Omar Ahmed Mohamed[1]

[1] *Faculty of Science, Engineering and Technology, Swinburne University of Technology, Victoria, Australia 3122*
[2] *Defence Materials Technology Centre, Victoria, Australia 3122*

Abstract

Selective Laser Melting (SLM) is a powder-bed type Additive Manufacturing (AM) process, where metal powder melting is followed by rapid solidification to yield metallic components. The mechanical performance of the components is greatly influenced by various SLM process parameters such as laser power, scan speed, scan pattern, hatch distance, build orientation, layer thickness and defocus distance. Studies on compressive properties of stainless steel parts by SLM have received relatively little attention. In this study, an investigation was conducted to assess the influence of laser power, build orientation, layer thickness and laser defocus distance on the mechanical behaviour of selective laser melted 17-4 PH stainless steel parts under quasi-static compression. Fractional factorial design was used to optimise the four process parameters to obtain maximum hardness and compressive strength with least porosity. Results are supported by studies on porosity and microstructure observations.

Keywords: Selective laser melting, 17-4 PH, Quasi-static compression, microhardness, factorial design

*Corresponding author: smasood@swin.edu.au

1. Introduction

Selective Laser Melting (SLM) is an additive manufacturing technique that can print almost fully dense metal parts from pre-alloyed materials such as 17-4 PH, AlSi12 and Ti6Al4V [1-4]. SLM can yield near net shaped components, which was reported by many authors [5-8]. The most common applications of SLM are in automotive and aerospace industry, where complex components can be produced, which are otherwise difficult through conventional methods [9]. The SLM process is a powder-bed type process, where metal powder is spread across the build plate and fused selectively with a high energy laser beam. The scanner scans a layer based on the computer aided design (CAD) geometry. The next layer is progressively scanned while the plate moves downwards equivalent to the layer thickness. In order to avoid the delamination of the built parts due to thermal stresses, parts are fabricated in a closed inert gas chamber.

Although SLM is effective in producing intricate and complex components for a wide number of applications, it is a very complex process due to the large number of process parameters

involved. The process parameters are broadly related to laser, atmosphere, temperature and metal powder [10]. The process parameters affect the microstructure as well as the mechanical properties of the built part [11-13]. Joguet et al [14] studied, where Taguchi method was applied for controlling the porosity content of titanium and CoCrMo parts, the SLM parameters namely hatch distance, point distance and exposure time were found to have the greatest influence on the process response. Song et al [11] investigated the influence of the process parameters including laser power and scanning speed on the microstructure of SLM built Ti6Al4V parts. These two parameters have significant influence on the microhardness as it is found that microhardness has a linear relationship with the densification in the compression testing of parts.

The 17-4 PH stainless steel is a precipitation hardened material with superior mechanical properties such as high tensile strength, toughness and good corrosive resistance. The 17-4 PH has found applications in aerospace, chemical and petrochemical industries. Recently Mahmoudi et al carried out a study [15] on SLM built 17-4 PH parts, the build orientation was found to have a direct effect on the mechanical properties of SLM parts, with vertical orientation exhibiting lower yield point. In that study, the post-SLM heat treatment of parts influenced the part strength and hardness positively but the ductility was found to be reduced. Also, the compressive yield strength was found to be 25% higher than the tensile yield strength. In the work by Yadollahi et al [16] on the mechanical and microstructural properties of selective laser melted 17-4 PH SS, a lower ductility was observed when compared to wrought alloy. The lower ductility was attributed to the presence of a large number of pores and un-melted powder particles. These pores were mainly due to the entrapped gases. Averyanova et al [17] have investigated the effect of main process parameters of selective laser melting (SLM) technology on single lines and single layers manufactured from 17-4 PH martensitic powder on hardness and track dimensions using the experimental design approach.

Previous literature indicates that little work has been done on the effect of SLM process parameters on the mechanical performance of 17-4 PH stainless steel parts produced by selective laser melting under compressive loading conditions. This paper is focussed on studying the effect of four key SLM parameters namely laser power, build orientation, layer thickness and laser defocus distance on the microhardness, ultimate strength, yield strength, porosity and stress-strain behaviour under compression of 17-4 PH samples made by SLM. In this paper, an experimental fractional factorial design approach has been applied to optimise the process parameters for the 17-4 PH parts. A comparison of compressive behaviour of SLM built 17-4 PH sample with wrought 17-4 PH sample is also presented.

2. Material and Methods

3D Systems ProX200 selective laser melting machine was used for manufacturing the 17-4 PH samples for quasi-static compression. The machine has a maximum laser power of 300 W and a work volume of 140 mm x 140 mm x 100 mm. The machine was operated under nitrogen protective atmosphere for the samples. The test samples were built in three different orientations as shown in Figure 1, where the inclined sample is at 45^{o} in X-Z plane. The cylindrical samples of size 13 mm diameter and 25 mm height, as shown in Figure 2, were tested as per ASTM E9 standard. The quasi-static compression tests were performed on the 250kN MTS universal testing machine at a deformation rate of 2 mm/min, with the strain rate of $4x\ 10^{-3}\ s^{-1}$, which is comparable to other reported values [16]. The force-displacement values were directly measured from the MTS250 compression machine and were used to plot stress-strain curves.

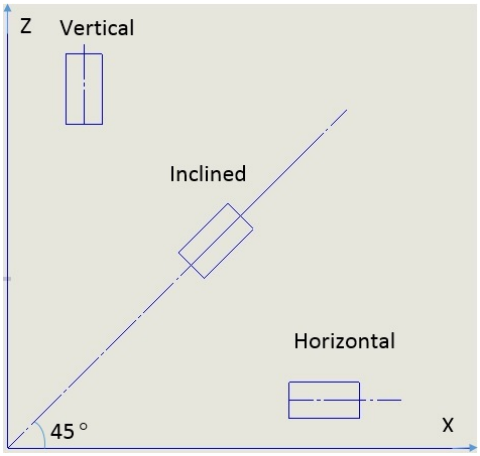

Figure 1 Build Orientations

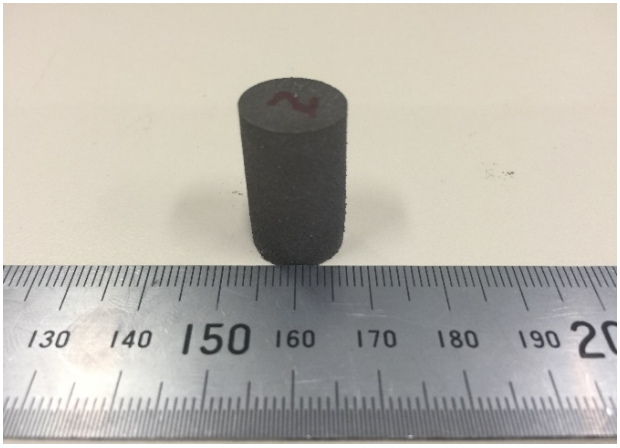

Figure 2 SLM built compression sample.

The microhardness of SLM samples were measured by Vickers Microhardness tester and an average of five measurements have been carried out. As per ASTM E 384 -11, hardness was measured using the diamond shaped indenter where the force applied was 300 gf and the dwelling time was 15 seconds. An experimental design approach using fractional orthogonal design based on Taguchi's design matrix is used in this study. Of the numerous parameters involved in the SLM process, four key parameters, namely laser power (A), build orientation (B), layer thickness (C) and defocus distance (D), and with three levels of values were used in this work as shown in Table 1. Two responses for mechanical performance, the microhardness and the ultimate compressive strength (UCS), were considered for fractional factorial design based on the Taguchi's method involving a total of nine tests. The porosity of SLM built samples was calculated based on relative density equation $RD = (1 - \rho 1/\rho 2)$, which is defined as the ratio of measured density to the theoretical density (7.8 g/cc) of the material.

Table1 Experimental design for the key SLM Parameters

Factors	**Parameter**	**Unit**	**Levels of each parameter**		
			Level 1	**Level 2**	**Level 3**
A	Laser Power (max 300 W)	W	240	255	270
B	Build Orientation	degree	0	45	90
C	Layer Thickness	µm	30	35	40
D	Defocus Distance	Mm	-6	-3	-1

3. Results and Discussion

Table 2 shows the results of the hardness and ultimate compressive strength (UCS), obtained from conducting 9 runs of experiments according to the experimental design plan for the four process parameters represented by factors A, B, C and D. The highest value of hardness is observed in test number 5 corresponding to 255 W laser power, 45° build orientation, 40 µm layer thickness and -6 mm defocus distance. Basically, the presence of martensite influences the microhardness positively, therefore it could be one of the reasons for the increase in microhardness. However, the test number 4 shows the least value of hardness that is attributed to the nitrogen atmosphere in the SLM build chamber that facilitates higher retained austenite than martensite. Also it could be due to the least amount of nitrogen flowing around the area of test sample 4 built area, which needs further evaluation [15]. Even though the hardness value is less in test no.1, it has the highest compressive strength, which could be attributed to the martensite formation. High solidification and cooling rates of the melt pool in SLM leads to the retained austenite formation. Eventually, as a known fact the retained austenite will induce ductility in the sample that could be observed in sample no.1.

Table 2 Experimental plan and its responses

Run	**Process Parameters**				**Average Micro hardness (+/- 2 HV)**	**Ultimate Compressive Strength**
	A	**B**	**C**	**D**	**HV**	**MPa**
1	80	0	30	-6	304	1132
2	80	0	35	-3	301	1053
3	80	0	40	-1	295	1053
4	85	45	35	-1	281	1076
5	85	45	40	-6	319	1028
6	85	45	30	-3	317	1046
7	90	90	40	-3	309	1064
8	90	90	30	-1	308	1043
9	90	90	35	-6	310	1059

3.1 Microhardness

The microhardness data was statistically analysed using Minitab version 17 and the main effects plot is presented in Figure 3. The laser power (A) has a direct influence on the hardness of the built part in the SLM. The increase in the laser power from 240 W to 270 W has a corresponding increase in the microhardness from 300 HV to 309 HV as observed in Figure 3. In this work, all the parts were built with the constant scanning speed of 2500 mm/s.

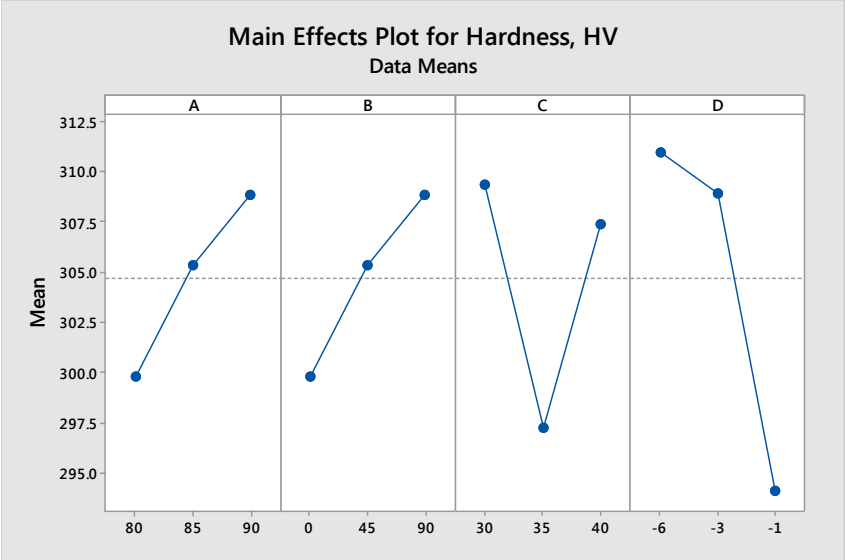

Figure 3 Influence of the four process parameters, Laser power (A), Build orientation (B) Layer thickness (C) and Defocus distance (D). on the microhardness of SLM 17-4 PH samples.

At 270 W of laser power, in the vertical orientation, at 30 µm layer thickness and with -6 mm defocus distance, one set of optimal conditions are arrived as shown in Figure 3, for improving the mechanical performance in terms of hardness.

While comparing the interactions between the build orientation (B) and layer thickness (C), the inclined orientation at 40 µm layer thickness is found to produce the hardness value of 318 HV. Also, at an inclined orientation of 45^0, with -6 mm defocus distance, the hardness obtained is 318 HV. Finally, in the interaction between the layer thickness (C) and defocus distance (D), the 40 µm layer thickness with -6 mm defocus distance is found to provide maximum hardness of 318 HV. As already explained, the rationale is the presence of martensite that makes the sample hard and brittle. The microhardness increases with decrease in layer thickness [18]. This could be due to the least layer thickness, which would enable nearly complete melting of metal powders [17].

3.2 Microstructure

Figure 4 shows the optical micrograph of the 17-4 PH SLM sample at two different magnifications. The SLM samples were polished and etched using Marble's reagent. An Olympus BX61 optical microscope was used to image the microstructure on the samples. The martensite structure is shown as grain and needle like structure without defined boundaries, which basically adds strength to the SLM made part in addition to the hardness. The measurements for retained

austenite grain size shows that in the lateral direction, the measured value is in the range from 40 µm to 55 µm and in the longitudinal direction, the value ranges from 70 µm to 100 µm. The calculated retained austenite area is more than the martensitic area and the value is 18.15 mm^2, where the total area is 32.14 mm^2, which is based on 20 measurements taken using spotcam software. On the one hand, retained austenite increases with increase in scanning speed and on the other hand retained austenite increases with decrease in laser power [19] . The pores shown in Figure 4 could be due to large thermal stresses [20]. Besides, the pores in the SLM built components could be due to entrapped gases, unmelted regions, and lack of fusion in the metal powder [16].

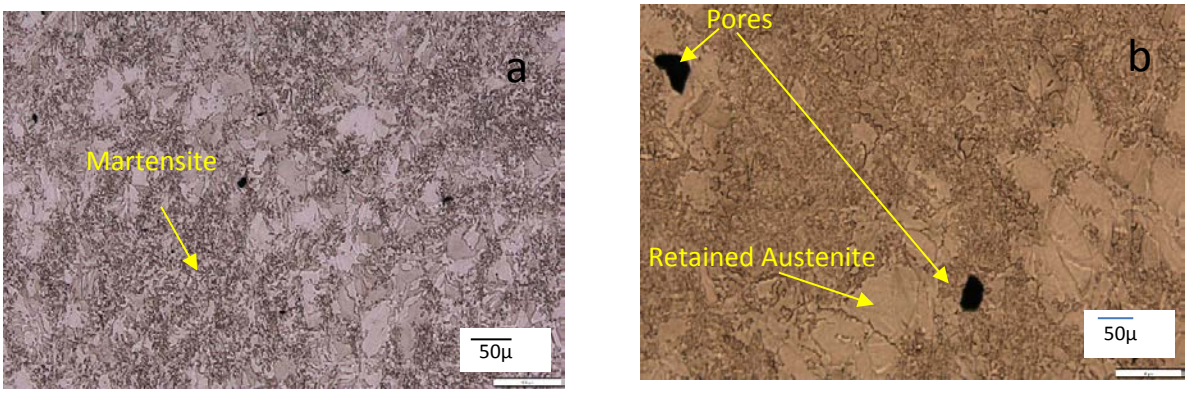

Figure 4 Optical micrograph of SLM produced17-4 PH sample at (a) 10X magnification and (b) 20X magnification.

The presence of retained austenite may have significant influence on microhardness. The amount of retained austenite may cause possible variation in the microhardness across the experimental plan [16]. Due to the increase in porosity, not only the hardness but also the relative density decreases. The dense needle like structure of martensite is generally hard by nature and adds strength to the SLM made 17-4 PH part. Also, the mechanical properties rely on microstructure, which in turn is dependent on thermal history of the built part.

3.3 Ultimate Compressive Strength

In Figure 5 shows the main effect plots for ultimate compressive strength (UCS) for SLM samples. It is observed that the samples exhibit the maximum compressive strength at 240 W laser power and at horizontal orientation. The laser has the sufficient power at 240 W laser power to melt the 17-4 PH metal powders nearly completely. Therefore, it is essential to increase the laser power only if it is required by the optimisation plot. Otherwise, increasing the laser power will lead to adverse effects such as balling and inconsistent melting in the melt pool. The main effects plot provides one of the optimum conditions where the laser power is 240 W of maximum power.

The build orientation in the horizontal orientation offers a rigid support, which enables to produce the part with maximum compressive strength. The layer thickness of 30 µm and the defocus distance of -6 mm are found to produce the maximum compressive strength. The layer thickness of the least value of 30 µm offers nearly complete melting [17].

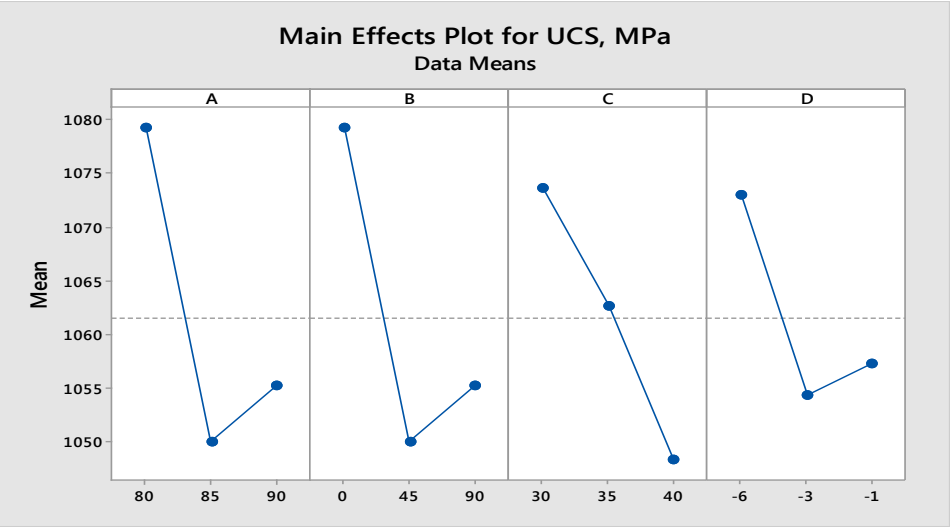

Figure 5 Influence of the process parameters , Laser power (A), Build orientation (B) Layer thickness (C) and Defocus distance (D), on the Ultimate Compressive Strength (UCS) of SLM 17-4 PH samples.

At 240 W laser power and horizontal orientation, the UCS is found to be 1132 MPa, which is the maximum. The support structures vary for each orientation therefore the laser power and UCS values may also vary. The maximum value achieved for UCS could be due to rigid support structure at horizontal orientation and the least laser power would be sufficient to melt the powders nearly complete. Therefore, nearly complete melting and rigid support enables the part to arrive at maximum compressive strength. Similarly, at 240 W laser power, the layer thickness of 30 µm and defocus distance of -6 mm, the UCS is observed to be one of the best values. The rationale could be that the least layer thickness could be melted completely to arrive at a dense part. In the interaction between build orientation and layer thickness, the horizontal orientation yields the maximum UCS, which is 1132 MPa against the least layer thickness of 30 µm. And, in the interaction between build orientation and defocus distance, it yields the maximum compressive strength due to martensitic structure in the microstructure, as explained earlier.

3.4 Comparison of Stress-Strain with Wrought 17-4 PH

Compressive test was also carried out for wrought 17-4 PH sample under the same test conditions as the SLM built 17-4 PH samples. Figure 6 shows a comparison of the stress strain curves of wrought sample with SLM built sample, which provided highest ultimate compressive strength (UCS) using the process parameter combination of 240 W laser power, horizontal orientation, 30-µm layer thickness and -6 mm defocus distance (test run 1). It is noticed that SLM made 17-4 PH sample provides much higher UCS (1132 MPa) and ductility compared to wrought 17-4 PH sample with a UCS of only 990 MPa. Moreover, all SLM samples tested in Table 2 show higher compressive strength compared to wrought sample tested. This higher ductility is mainly due to the retained austenite in the SLM built samples.

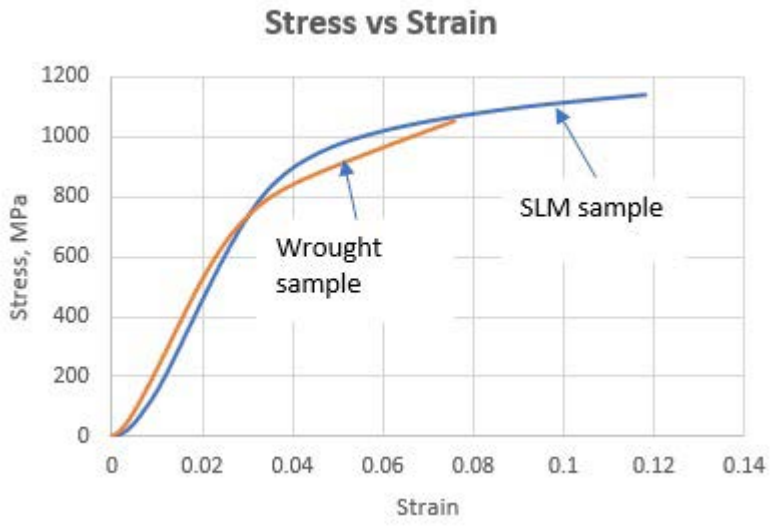

Figure 6 Stress vs Strain curves for wrought 17-4 PH sample and SLM built 17-4 PH sample

3.5 *Yield Strength*

Figure 7 shows the variation of yield strength (YS) for all nine test runs as shown in Table 2. Sample run 1 shows the highest yield strength of 900 MPa with the parameters combination of 240 W of maximum laser power, horizontal orientation, the 30 µm layer thickness and -6 mm defocus distance. This would provide better mechanical performance of the 3D printed 17-4 PH sample. Both the UCS and YS are found to be maximum for the same combination of process parameters due to the hard and brittle martensitic phase as referred to in section 3.2.

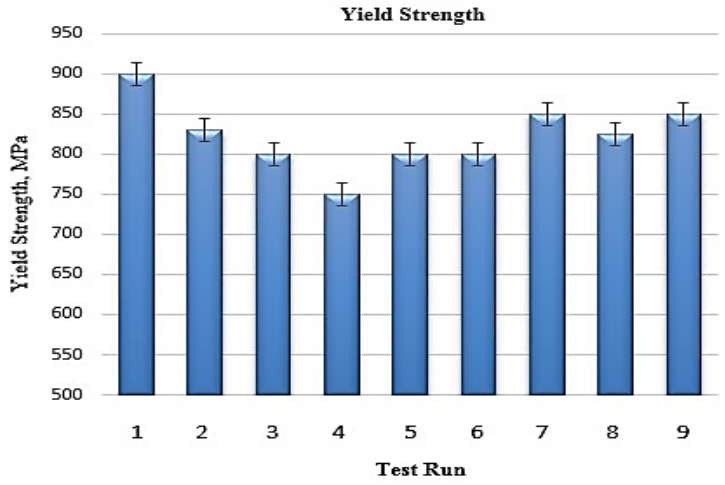

Figure 7 Yield Strength of 17-4 PH SLM samples

3.6 *Porosity*

Figure 8 shows the percentage porosity for each of the nine test samples. It is noted that sample 5, with process parameters of 255 W of maximum laser power, 45^0 build orientation, 40 µm layer thickness and -6 mm defocus distance, had the maximum amount of porosity of 4.69%. However, sample 6 shows the least porosity of 2.85% with the process parameters of 255 W of maximum laser power, 45^0 build orientation, 30 µm layer thickness and -3 mm defocus distance. Therefore, this parameter group is one such parameter combination that could provide the least porosity and also improve mechanical performance. The melt pool behaviour influences the porosity of the sample to a greater extent. Especially the combination of laser power and scanning speed affects the melt pool behaviour significantly.

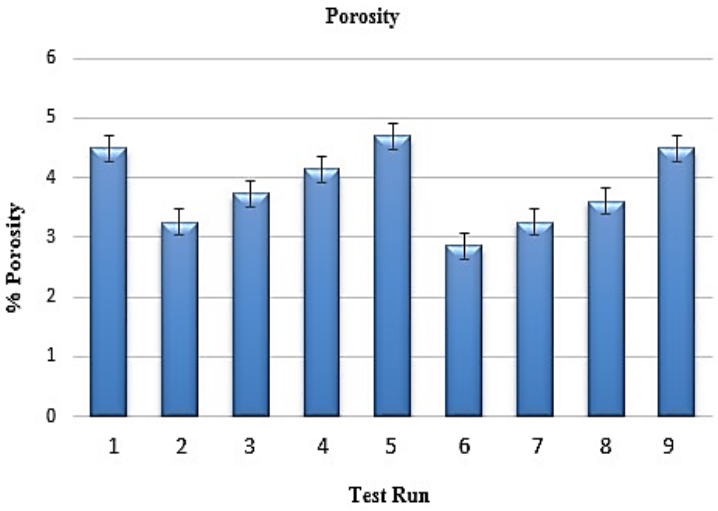

Figure 8 Porosity of 3D printed 17-4 PH SLM samples.

3.7 *Optimisation*

The optimization of process parameters was done using the response optimiser in Minitab 17 to arrive at the maximum hardness and maximum ultimate compressive strength. Figure 9 represents the optimization plot for the optimal conditions for generalized responses. Minitab computes the optimal setting for the input parameters along with overall composite desirability value to demonstrate how well the optimal setting achieves the response criteria. Based on Figure 9, in order to achieve maximum hardness and maximum ultimate compressive strength simultaneously, it is essential to follow the optimal processing conditions. The set of conditions required for strengthening the part hardness and ultimate compressive strength simultaneously are found to be 270 W laser power, vertical orientation, 30 µm layer thickness and -6 mm defocus distance with the composite desirability of 0.6349, which indicates that the acceptable compressive performance within 0.8 composite desirability could be achieved.

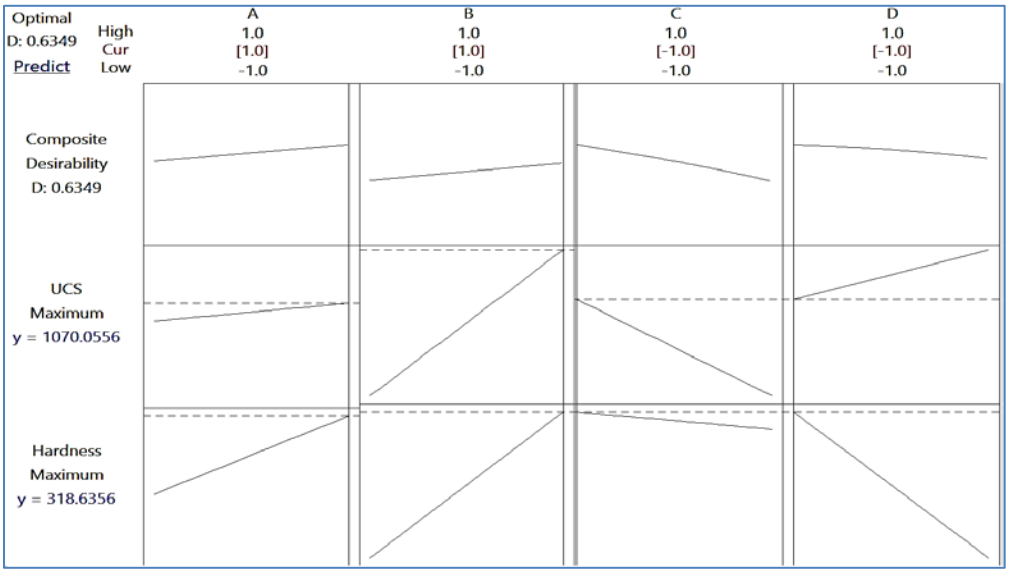

Figure.9 Optimisation of process parameters.

4. Conclusions

The statistical analysis of microhardness and ultimate compressive strength were performed, where the main effects plot are analysed along with the optimisation chart. Based on the optimisation plot, it could be observed that 270 W laser power, vertical orientation, 30 µm layer thickness and -6 mm defocus distance is one set of results with which improved mechanical performance could be achieved. The martensitic structure adds both hardness as well as strength to the SLM produced 17-4 PH part. The area of the retained austenite is higher than the martensite area whose values are 18.15 mm^2 and 13.99 mm^2 respectively, as the shielding gas used is nitrogen.

Acknowledgements

The authors gratefully acknowledge the support of Defence Materials Technology Centre (DMTC), Melbourne, Australia.

References

[1] Kruth J-P, Froyen L, Van Vaerenbergh J, Mercelis P, Rombouts M, Lauwers B. Selective laser melting of iron-based powder. Journal of Materials Processing Technology. 2004;149(1):616-22.

[2] Thijs L, Kempen K, Kruth J-P, Van Humbeeck J. Fine-structured aluminium products with controllable texture by selective laser melting of pre-alloyed AlSi10Mg powder. Acta Materialia. 2013;61(5):1809-19.

[3] Rombouts M, Kruth J-P, Froyen L, Mercelis P. Fundamentals of selective laser melting of alloyed steel powders. CIRP Annals-Manufacturing Technology. 2006;55(1):187-92.

[4] Louvis E, Fox P, Sutcliffe C J. Selective laser melting of aluminium components. Journal of Materials Processing Technology. 2011;211(2):275-84.

[5] Yadroitsev I, Bertrand P, Smurov I. Parametric analysis of the selective laser melting process. Applied surface science. 2007;253(19):8064-9.

[6] Yadroitsev I, Shishkovsky I, Bertrand P, Smurov I. Manufacturing of fine-structured 3D porous filter elements by selective laser melting. Applied Surface Science. 2009;255(10):5523-7.
[7] Xu W, Brandt M, Sun S, Elambasseril J, Liu Q, Latham K, Xia K, Qian M. Additive manufacturing of strong and ductile Ti–6Al–4V by selective laser melting via in situ martensite decomposition. Acta Materialia. 2015;85:74-84.
[8] Kempen K, Thijs L, Van Humbeeck J, Kruth J-P. Mechanical properties of AlSi10Mg produced by selective laser melting. Physics Procedia. 2012;39:439-46.
[9] Aboulkhair N T, Maskery I, Tuck C, Ashcroft I, Everitt N M. The microstructure and mechanical properties of selectively laser melted AlSi10Mg: the effect of a conventional T6-like heat treatment. Materials Science and Engineering: A. 2016;667:139-46.
[10] Kurzynowski T, Chlebus E, Kuźnicka B, Reiner J, editors. Parameters in selective laser melting for processing metallic powders. SPIE LASE; 2012: International Society for Optics and Photonics.
[11] Song B, Dong S, Zhang B, Liao H, Coddet C. Effects of processing parameters on microstructure and mechanical property of selective laser melted Ti6Al4V. Materials & Design. 2012;35:120-5.
[12] Thijs L, Verhaeghe F, Craeghs T, Van Humbeeck J, Kruth J-P. A study of the microstructural evolution during selective laser melting of Ti–6Al–4V. Acta Materialia. 2010;58(9):3303-12.
[13] Vrancken B, Thijs L, Kruth J-P, Van Humbeeck J. Heat treatment of Ti6Al4V produced by Selective Laser Melting: Microstructure and mechanical properties. Journal of Alloys and Compounds. 2012;541:177-85.
[14] Joguet D, Costil S, Liao H, Danlos Y. Porosity content control of CoCrMo and titanium parts by Taguchi method applied to selective laser melting process parameter. Rapid Prototyping Journal. 2016;22(1):20-30.
[15] Mahmoudi M, Mahmoudi M, Elwany A, Elwany A, Yadollahi A, Yadollahi A, Thompson S M, Thompson S M, Bian L, Bian L. Mechanical properties and microstructural characterization of selective laser melted 17-4 PH stainless steel. Rapid Prototyping Journal. 2017;23(2):280-94.
[16] Yadollahi A, Shamsaei N, Thompson S M, Elwany A, Bian L, editors. Mechanical and microstructural properties of selective laser melted 17-4 PH stainless steel. ASME 2015 International Mechanical Engineering Congress and Exposition; 2015: American Society of Mechanical Engineers.
[17] Averyanova M, Cicala E, Bertrand P, Grevey D. Experimental design approach to optimize selective laser melting of martensitic 17-4 PH powder: part I-single laser tracks and first layer. Rapid Prototyping Journal. 2012;18(1):28-37.
[18] Krishnan M, Atzeni E, Canali R, Calignano F, Manfredi D, Ambrosio E P, Iuliano L. On the effect of process parameters on properties of AlSi10Mg parts produced by DMLS. Rapid Prototyping Journal. 2014;20(6):449-58.
[19] Kwok C, Leong K, Cheng F, Man H. Microstructural and corrosion characteristics of laser surface-melted plastics mold steels. Materials Science and Engineering: A. 2003;357(1):94-103.
[20] Monroy K, Delgado J, Ciurana J. Study of the pore formation on CoCrMo alloys by selective laser melting manufacturing process. Procedia Engineering. 2013;63:361-9.